Available online at www.sciencedirect.com

SCIENCE DIRECT®

European Journal of Pharmaceutics and Biopharmaceutics 60 (2005) 113–122

European Journal of Pharmaceutics and Biopharmaceutics

www.elsevier.com/locate/ejpb

Research paper

Novel nanoparticulate carrier system based on carnauba wax and decyl oleate for the dispersion of inorganic sunscreens in aqueous media

J.R. Villalobos-Hernández, C.C. Müller-Goymann*

Institut für Pharmazeutische Technologie, Technische Universität Braunschweig, Braunschweig, Germany

Received 18 August 2004; accepted in revised form 19 November 2004
Available online 13 January 2005

Abstract

The purpose of this study was to characterize carrier systems for inorganic sunscreens based on a matrix composed of carnauba wax and decyl oleate. Ultraviolet radiation attenuators like barium sulfate, strontium carbonate and titanium dioxide were tested. The lipid matrices were used either as capsules or as accompanying vehicles for the pigments in aqueous dispersions. Manufacturing was performed using high pressure homogenization at 300 bar and a temperature of 75 °C. To evaluate the effect of the pigments on the crystalline structure of the wax–oil mixture, X-ray diffraction and differential scanning calorimetry were used. Further parameters determined were particle size, polydispersity index, *z*-potential, viscosity and sun protection factor (SPF). Transmission electron microscopy was also applied for visualization of nanoparticles. The X-ray diffraction patterns and the melting points of the lipid mixtures remained unchanged after the pigments were added. The particle sizes of the encapsulated species ranged from 239 to 749.9 nm showing polydispersity values between 0.100 and 0.425. Surface charge measurements comprising values up to −40.8 mV denoted the presence of stable dispersions. The formulations could be described as ideal viscous presenting viscosities in a range of 1.40–20.5 mPa s. Significant increases in SPF up to about 50 were reported after the encapsulation of titanium dioxide. Freeze fracture micrographs confirmed the presence of encapsulated inorganic crystals.

Keywords: Nanoparticulate carriers; High pressure homogenization; Inorganic sunscreens; Carnauba wax; Decyl oleate; Sun protection factor

1. Introduction

Originally used as longer sun exposure enablers and tanning promoters, sunscreens are now recommended for preventing skin cancer, accelerated skin aging and other cutaneous changes including pigmentation anomalies [1]. The ultraviolet radiation attenuation of inorganic sunscreens is known to occur, depending on the nature of the compound, by three mechanisms namely scattering, reflection and absorption. Examples of compounds attenuating ultraviolet radiation mainly by scattering and reflection are barium sulfate and talc [2]. There are many other inorganic salts remaining to this classification, but in some cases, their potential use in sun protection products has not been evaluated, e.g. strontium carbonate [3–5]. Inorganic sunscreens also exhibit non-specific UV wavelength absorption. Their mechanism of UV absorption involves the use of photon energy to excite electrons at wavelengths, depending on the compound, in the range of sun protection (280–400 nm) [6]. For this reason, these substances are recognized as effective ingredients in sun screening formulation, being titanium dioxide and zinc oxide the most typical representatives of this class [7,8].

To incorporate inorganic filters into sunscreen products, it is a common practice to mix them with liquid lipids before being distributed in o/w emulsions. But, in those cases, the formulations generally require high concentrations of pigments or the combination with many other substances to obtain an acceptable sun protection factor [9]. In order to increase the efficiency and efficacy of sunscreens, suitable carrier systems have to be developed. Nowadays, inorganic

---

* Corresponding author. Address: Institut für Pharmazeutische Technologie, Technische Universität Braunschweig, Mendelssohnstrabe 1, D-38106 Braunschweig, Germany. Tel.: +49 531 391 5650; fax: +49 531 391 8108.

E-mail address: c.mueller-goymann@tu-bs.de (C.C. Müller-Goymann).

0939-6411/$ - see front matter © 2004 Elsevier B.V. All rights reserved.
doi:10.1016/j.ejpb.2004.11.002

compounds can be easily produced in nanoscale and treated to modify their surfaces so that they acquire hydrophobic properties [10]. Moreover, the small crystal size and the controlled particle size distribution of such products enable a good dispersion in different media. Solid lipid nanoparticles could be appropriate vehicles to carry inorganic pigments. Nevertheless, these systems generally exhibit a lack of drug load capacity and thus a drug expulsion during storage [11,12]. To overcome such phenomena, the application of a binary mixture between a thermoplastic lipid and a liquid lipid to encapsulate inorganic pigments is purposed in this work. The lipid mixture could avoid the crystal arrangement of the wax after solidification, by which the drug expulsion takes place as observed by Müller et al. and Jenning et al. [13,14]. Carnauba wax is described as a plastic solid obtained from the carnauba palm tree. It is a very hard material having a melting point range from 81 to 86 °C and consisting of a complex mixture of high molecular weight esters of acid and hydroxyacids [15]. Decyl oleate is a well known emollient showing high fluidity and causing no irritation when it is spread onto human skin [16]. According to this, the combination of the properties of both excipients constitutes a potential medium for the dermal application of inorganic sunscreens. One possibility to reach this aim is their integration into nanoparticles by means of high pressure homogenization (HPH) [17]. These novel particles might enhance the UV attenuation of the inorganic sunscreens not only by the scattering attributed to the increase in number of solid species showing particle sizes in nanodimension, but also by the augmented UV absorption in virtue of the compounds present in the complex mixture of the carnauba wax. Furthermore, the new formed vehicles could provide the inorganic crystals with a support structure for a better fixation when applied onto skin.

It was the objective of this study to develop lipid matrices consisting of carnauba wax and decyl oleate by dint of HPH for the encapsulation of inorganic sunscreens such as barium sulfate, strontium carbonate and titanium dioxide. To achieve this goal, the study included an evaluation of the raw materials and mixtures thereof using X-ray diffraction and differential scanning calorimetry to appreciate possible changes in the crystalline structure of the mixture wax–oil after the incorporation of the inorganic species. Subsequently, the lipid matrices containing pigments were dispersed into aqueous media constituting nanosuspensions being later characterized considering different physicochemical and technological parameters, i.e. particle size, polydispersity index, *z*-potential, viscosity and sun protection factor. To set a comparison, unloaded lipid matrices and freely dispersed pigment nanosuspensions were also prepared and evaluated regarding the same parameters. In the case of titanium dioxide, a well known good inorganic sunscreen [18], special preparations containing a mixture of lipid matrices and pigment crystals were made, and their properties could be compared with those of the formulations containing encapsulated species. By doing all the above, a better description of the performance of the formulations as possible sun protectors could be established, and finally, in order to get a closer approach of these novel structures, transmission electronic microscopy was applied.

2. Materials and methods

2.1. Materials

The following materials were obtained from the indicated sources: Alumina–stearic acid surface treated nanofine titanium dioxide having a primary particle size (PPS) of about 17 nm (Kemira, Finland), nanofine barium sulfate (PPS ca. 30 nm) (Solvay, Germany), strontium carbonate (PPS ca. 30 nm) (Solvay, Germany), carnauba wax Ph. Eur. (Caelo, Germany), decyl oleate (Caelo, Germany), Tween® 80 (Atlas Chemie, Germany), simethicone antifoamer (Sigma Aldrich, Germany) and methylisothiazolinone (Brenntag, Germany). Bidistilled and filtered water (0.2 μm) was used for each preparation.

3. Experimental methods

3.1. Nanosuspensions containing encapsulated pigments

The nanosuspensions were produced by dispersing a lipid phase in an aqueous phase using high pressure homogenization. The lipid phase were composed of carnauba wax, decyl oleate and pigment as indicated in Table 1. Those substances were mixed together by melting the wax at 90 ± 5 °C and applying magnetic stirring during 30 min at a rate of 300 rpm. The aqueous phase was prepared by dispersing the components as expressed in Table 1 at a speed rate of 300 rpm. Both phases were initially pre-dispersed by using high shear dispersion system, Ultraturrax® (IKA, Germany) at 26,000 rpm during 5 min at a temperature of 90 ± 5 °C. The loss of water was compensated and the obtained dispersions were homogenized under temperature 75 ± 5 °C at a pressure of 300 ± 10 bar within 30 passes. A Niro

Table 1
Chemical composition and concentration of constituents in nanosuspension formulations containing encapsulated pigments

Substances	w/w (%)
Lipid phase	
Pigment: TiO_2, $BaSO_4$ or $SrCO_3$	2, 4, 6
Decyl oleate	5
Carnauba wax	5, 10
Aqueous phase	
Tween 80	1
Simethicone	0.01
Methylisothiazoline	0.0285
Double distilled and filtered water	q. s. 100

Table 2
Chemical composition and concentration of constituents in nanosuspension formulations containing carnauba wax–decyl oleate (wax–oil) nanoparticles

Substances	w/w (%)
Lipid phase	
Decyl oleate	5
Carnauba wax	5, 10
Aqueous phase	
Tween 80	1
Simethicone	0.01
Methylisothiazoline	0.0285
Double distilled and filtered water	q. s. 100

homogenizer Typ II (Niro, Italy) was used for this purpose. Methylisothiazolone was added as preservative at room temperature at the end of the process. For comparative purposes and following the aforementioned manufacturing procedure, carnauba wax–decyl oleate particle dispersions containing no pigments were also prepared. Formulations can be appreciated in Table 2.

3.2. Nanosuspensions containing inorganic species without carnauba wax and decyl oleate

To evaluate the performance of the pigments without the effect of the capsule forming lipids, pigment suspensions made of $BaSO_4$, $SrCO_3$ and TiO_2 were prepared. The formulations can be observed in Table 3. In these cases, the crystals were dispersed in the aqueous phase by high shear stirring at 26,000 rpm during 5 min. The dispersions were subsequently homogenized applying 300 ± 10 bar at room temperature during 30 passes.

3.3. Nanosuspensions containing non-encapsulated titanium dioxide

In the case of titanium dioxide, the formulations having freely dispersed crystals in the presence of lipid nanoparticles were prepared according to the compositions shown in Table 4. Wax–oil dispersions were made by high pressure homogenization as described before (see Section 3.1) and cooled down to room temperature. Titanium dioxide crystals were carefully added and pre-dispersed by stirring at 26,000 rpm during 5 min. For the final dispersions, high pressure homogenization of 300 ± 10 bar at room temperature within 30 passes was applied.

Table 3
Chemical composition and concentration of constituents in nanosuspension formulations containing pigments without capsule forming lipids

Substances	w/w (%)
Pigment: TiO_2, $BaSO_4$ or $SrCO_3$	2, 4, 6
Tween 80	1
Simethicone	0.01
Methylisothiazoline	0.0285
Double distilled and filtered water	q. s. 100

Table 4
Chemical composition and concentration of constituents in nanosuspension formulations containing wax–oil nanoparticles and non-encapsulated titanium dioxide

Substances	w/w (%)
Lipid phase	
Decyl oleate	5
Carnauba wax	5, 10
Aqueous phase	
Pigment: TiO_2	2, 4, 6
Tween 80	1
Simethicone	0.01
Methylisothiazoline	0.0285
Double distilled and filtered water	q. s. 100

3.4. X-ray diffraction

Wide angle X-ray diffraction (WAXD) diagrams of bulk materials and their mixtures obtained after melting and recrystalization were measured using a Goniometer PW1710-S (Philips, The Netherlands). Samples were placed on aluminium plates and the Bragg's angle was obtained from the diffraction pattern.

3.5. Differential scanning calorimetry

Thermal behaviour studies were performed using a calorimeter DSC 220 C (Seiko, Japan). Approximately 5 mg of bulk materials and their mixtures were tested. The probes were scanned in a temperature range of −20 to 150 °C applying a heating rate of 5 °C/min.

3.6. Photon correlation spectroscopy (PCS) and polydispersity index (PI)

The particle diameters and polydispersity indices were simultaneously measured by PCS using a Zetasizer 3 (Malvern, Germany) modified with an He/Ne laser model 127 (Spectra Physics, USA). The detection was performed at 90° in a cell AZ 10 equilibrated at 293 K. The samples were diluted with filtrated double distilled water to provide recommended scattering activity. Three samples of each preparation were used and every sample was measured twice.

3.7. Transmission electron microscopy (TEM)

Samples for morphological examination were obtained by freeze fracturing at −100 °C at a pressure of 5×10^{-6} bar in a BAF 400 device (Balzers, Germany). Samples were shadowed with platinum/carbon (layer thickness 20 nm) at 45° and stabilized with carbon (layer thickness 20 nm) at 90°. Replicas were cleaned with sulphuric acid and viewed with a TEM JEM 3000 F (Jeol, USA) at 125 kV.

3.8. Z-Potential

The *z*-potential was determined by laser doppler velocimetry with Zetamaster model Z 5002 (Malvern, UK). Electrophoretic velocity was transformed into *z*-potential according to Helmholtz–Smoluchowski Eq. (1)

$$\mathrm{ZP} = \mathrm{EM} \times 4\pi\eta/\varepsilon \qquad (1)$$

ZP, *z*-potential; EM, electrophoretic mobility; η, viscosity of the dispersion medium; ε, dielectric constant and 4π, constant. The field strength applied was 30 V cm^{-1}, the conductivity was 0.5 mS cm^{-1}, and the measuring cell was 50 mm length, 2 mm height and 5 mm width. Samples were shaken and diluted with a 10^{-3} M NaCl solution and if necessary adjusted at pH of 7.4 using NaOH. The *z*-potential values were calculated and corrected for a standard reference temperature of 20 °C. Three samples of each preparation were determined.

3.9. Viscosity

Rheograms and viscosity measurements were performed by means of a Rheometer (Bohlin Inst., Germany) fitted with a 4 cm metallic parallel plate with a gap of 1 mm. Two non-diluted samples of every suspension were applied and measured at 20±0.1 °C.

3.10. In vitro sun protection factor (SPF)

The sun protection factor of every nanosuspension was measured by means of a SPF-290 analyzer (Optometrics Corp, UK). One hundred and ten microlitres-samples were spread over Transpore® tapes (3M GmbH, Germany) having an area of 55.5 cm^2. Radiation attenuation by the applied samples were performed in a wavelength range of 290–400 nm. Measurements of each formulation were taken in duplicate.

4. Results and discussion

4.1. Physicochemical characterization of bulk material and mixtures

To elucidate the effect of the pigments on the structure of the lipid matrix, X-ray diffraction studies were performed. The diffraction patterns of carnauba wax, a binary mixture of carnauba wax and decyl oleate (1:1), and ternary mixtures composed of wax, oil and pigment (1:1:0.38) were compared. The results are expressed in Table 5. Carnauba wax showed three typical diffraction bands at 2.9×10^{-1}, 3.7×10^{-1} and 4.1×10^{-1} nm in the wide angle region. A small modification of this pattern attributed to decyl oleate was observed in the binary mixture. This was identified by an additional signal at 4.5×10^{-1} nm. The ternary mixtures exhibited essentially the same diffraction pattern as the binary mixture, being only slightly modified by the presence of pigments as denoted by the reflections between 2.5×10^{-1} and 3.9×10^{-1} nm. The aforementioned results could be supported by the melting temperatures obtained by calorimetry scannings exposed in the same table. It can be appreciated that carnauba wax in the presence of decyl oleate presented a melting point of 78.5 °C and no significant change in this value after the addition of inorganic compounds to this mixture was reported.

Table 5
The main interlayer spacings (*d*) determined by X-ray diffraction and the melting points (T_m) of the bulk compounds and their mixtures

	CW	CW:DO (1:1)	CW:DO:$BaSO_4$ (1:1:0.38)	BaSO4	CW:DO:$SrCO_3$ (1:1:0.38)	$SrCO_3$	CW:DO:TiO_2 (1:1:0.38)	TiO_2
d	–	4.5	4.5	–	4.5	–	4.5	–
	–	–	4.4	–	–	–	–	–
	–	–	4.3	–	–	–	–	–
	4.1	–	–	–	4.1	–	4.1	–
	–	4.0	4.0	–	–	–	–	–
	–	–	–	–	–	–	–	3.9
	–	–	3.8	3.8	–	–	–	–
	3.7	–	3.7	3.7	3.7	–	–	–
	–	3.6	–	–	3.6	–	3.6	3.6
	–	–	3.5	3.5	3.5	3.5	–	–
	–	–	3.4	3.4	–	–	–	–
	–	–	–	3.3	–	–	–	–
	–	–	3.2	–	–	–	3.2	3.2
	–	–	3.0	3.0	–	3.0	–	–
	2.9	2.9	–	–	2.9	2.9	2.9	–
	–	–	2.8	2.8	2.8	2.8	–	–
	–	–	2.7	–	–	–	–	–
	–	–	–	2.5	–	2.5	–	2.5
T_m	83.5	78.5	77.8	–	77.3	–	76.9	–

Distances and melting points are expressed in 10^{-1} nm and °C, respectively. CW, carnauba wax; DO, decyl oleate.

Table 6
Mean particle sizes (PS ± SD) and polydispersity indices (PI ± SD) of the obtained nanosuspensions

Pigment	Pigment content (%)	Carnauba wax–decyl oleate ratio					
		0:0		1:1		2:1	
		PS (nm)	PI	PS (nm)	PI	PS (nm)	PI
None	0	–	–	244.0 ± 4.4	0.096 ± 0.056	319.0 ± 5.6	0.100 ± 0.063
$BaSO_4$ (E)	2	135.0 ± 3.1	0.175 ± 0.020	221.9 ± 4.0	0.136 ± 0.054	415.6 ± 15.6	0.243 ± 0.023
	4	147.0 ± 3.7	0.169 ± 0.041	254.1 ± 5.0	0.141 ± 0.066	412.9 ± 13.0	0.252 ± 0.031
	6	157.4 ± 2.2	0.170 ± 0.090	362.2 ± 13.8	0.247 ± 0.032	416.8 ± 22.4	0.249 ± 0.046
$SrCO_3$ (E)	2	1068.1 ± 178.2	0.577 ± 0.294	249.2 ± 4.0	0.170 ± 0.027	347.2 ± 12.3	0.083 ± 0.047
	4	1163.0 ± 130.3	0.758 ± 0.116	277.8 ± 4.6	0.230 ± 0.023	395.3 ± 12.4	0.295 ± 0.054
	6	1228.8 ± 135.6	0.498 ± 0.247	277.3 ± 10.4	0.218 ± 0.073	416.9 ± 7.0	0.106 ± 0.109
TiO_2 (E)	2	239.0 ± 10.0	0.215 ± 0.045	446.8 ± 24.4	0.313 ± 0.053	543.2 ± 28.0	0.298 ± 0.062
	4	255.5 ± 8.6	0.248 ± 0.020	460.8 ± 25.0	0.323 ± 0.053	717.7 ± 57.4	0.400 ± 0.057
	6	337.9 ± 17.8	0.298 ± 0.031	466.8 ± 17.7	0.310 ± 0.161	772.9 ± 66.3	0.417 ± 0.080
TiO_2 (NE)	2	See TiO_2 (E)	See TiO_2 (E)	296.3 ± 3.6	0.154 ± 0.037	336.6 ± 7.0	0.203 ± 0.065
	4			361.1 ± 9.1	0.231 ± 0.060	453.6 ± 24.8	0.413 ± 0.047
	6			453.6 ± 26.9	0.405 ± 0.339	749.9 ± 107.1	0.618 ± 0.425

E, encapsulated; NE, non-encapsulated.

4.2. Evaluation of nanosuspensions

4.2.1. Particle size and polydispersity indices

The mean particle sizes and the polydispersity indices of the freely dispersed pigments suspensions, the pigment-free lipid nanosuspensions, and the pigment-loaded lipid nanosuspensions are shown in Table 6. Since inorganic pigments were dispersed within a lipid matrix composed of carnauba wax and decyl oleate, these compounds are supposed to be encapsulated (E). Conversely, those pigments being added after the formation of carnauba wax–decyl oleate nanoparticles are identified as non-encapsulated (NE). The particle sizes of the freely dispersed pigments were evaluated, and in all the cases, they were different from the primary particle sizes of the pigments (c.f. Section 2). This can be explained through the agglomeration those compounds undergo either before or during the manufacturing process, especially when the loads of those compounds are increased. It has to be noticed that the particles containing crystals of barium sulfate or strontium carbonate exhibited similar mean particle sizes after they were encapsulated. Their values were found between 221 and 417 nm. The corresponding mean particle sizes of encapsulated titanium dioxide pigments were larger than those obtained with the other pigments, being the range in size from 446 to 772.9 nm. On the whole, the more the pigment and carnauba wax loads, the higher the particles sizes. In the case of titanium dioxide, the NE nanosupensions exhibited smaller mean particle sizes in comparison to those of the corresponding E formulations. Similar values from approximately 750 nm in both processes were only found when the highest concentration of pigment was applied. The increase in particle sizes can be attributed to association phenomena between pigment agglomerates and lipid particles. The polydispersity index (PI), on its side, indicates a measure of the width of the dispersion. According to Müller and Schumann [19], narrow dispersions comprise PI values between 0.1 and 0.2, meanwhile broad dispersions are reflected by PI values between 0.2 and 0.5, i.e. the pigment free lipid nanosuspensions were the only preparations giving narrow dispersions, meanwhile the rest of the dispersions were labeled as broad disperse and an increase of the PI values was seen when high loads of pigment and carnauba wax were used.

4.2.2. Surface charge measurements

Z-Potential is a useful parameter to estimate the stability of dispersed systems, the performed measurements are indicated in Table 7. All the formulations exhibited negative values. According to Riddick [20], *z*-potential values ≤ −21 mV are considered as advisable for the stabilization of dispersions, since very little or no agglomeration takes

Table 7
Z-Potential values ± SD (mV) of the obtained nanosuspensions

Pigment	Carnauba wax–decyl oleate ratio			
	Pigment content (%)	0:0	1:1	2:1
None	0		−29.2 ± 0.20	−36.9 ± 0.60
$BaSO_4$ (E)	2	−27.5 ± 0.40	−29.1 ± 1.20	−31.8 ± 0.10
	4	−33.4 ± 0.40	−31.3 ± 0.30	−34.0 ± 0.40
	6	−34.3 ± 0.50	−30.2 ± 0.50	−35.1 ± 0.40
$SrCO_3$ (E)	2	−21.5 ± 0.50	−43.4 ± 0.90	−43.0 ± 0.40
	4	−21.1 ± 0.30	−39.2 ± 1.50	−42.3 ± 1.80
	6	−21.9 ± 0.10	−37.3 ± 0.50	−40.8 ± 1.60
TiO_2 (E)	2	−5.7 ± 0.50	−20.1 ± 0.40	−23.6 ± 0.01
	4	−6.0 ± 0.20	−19.4 ± 0.40	−22.4 ± 0.70
	6	−5.7 ± 0.90	−18.4 ± 0.60	−21.7 ± 0.30
TiO_2 (NE)	2	See TiO_2 (E)	−27.9 ± 0.90	−35.9 ± 0.60
	4		−36.8 ± 0.50	−36.2 ± 0.40
	6		−31.9 ± 0.60	−32.7 ± 0.30

E, encapsulated; NE, non-encapsulated.

place. In terms of the latter, most of the dispersions were considered to be stable. On the contrary, the systems showing values tending to zero (higher than −21 mV) might present different grades of agglomeration, e.g. the freely dispersed titanium dioxide. Regarding the encapsulated particles, particularly extraordinary stable *z*-potential values were obtained after the encapsulation of strontium carbonate; barium sulfate preparations showed acceptable values, meanwhile titanium dioxide presented the lowest ones. In contrast to this, the non-encapsulated titanium dioxide crystals seemed to favor the dispersion of the wax–oil particles. In all the cases, a tendency to improve the stability of the dispersion was observed when the crystals were encapsulated into matrices having more wax content. Therefore, it could be assumed that larger carnauba wax loads for encapsulation or for dispersion of pigments contributed to improve the stability of each formulation.

4.2.3. Viscosity

Rheology describes the deformation and flow properties of matter. Viscosity is generally used to characterize the rheological behavior of liquids and suspensions. To evaluate this parameter in the produced nanoparticle suspensions, the relationship between shear rate (γ) and shear stress (σ) or reciprocal of viscosity ($1/\eta$) was plotted by means of a rotational viscometer. All preparations exhibited a linear behavior, and consequently can be referred as Newtonian fluids [21], some examples are depicted in Fig. 1 and are described according to the Eq. (2)

$$1/\eta = \gamma/\sigma \qquad (2)$$

It can be observed that the addition of wax–oil nanoparticles to the systems acting as pigment capsules or as dispersion media results in a viscosity increase. The corresponding viscosity values were plotted versus the carnauba wax–decyl oleate ratios as described in Fig. 2. For the encapsulated species, the increase in viscosity was observed when the highest wax–oil ratio was applied, whereas for the non-encapsulated species, only small increments were reported. The explanation must be mainly attributed to the modification of the wax–oil matrices after the inclusion of inorganic pigments, which caused not only an increase in size and weight, but also a change in the surface repulsion forces necessary to achieve the stabilization accounted for the *z*-potential values [22].

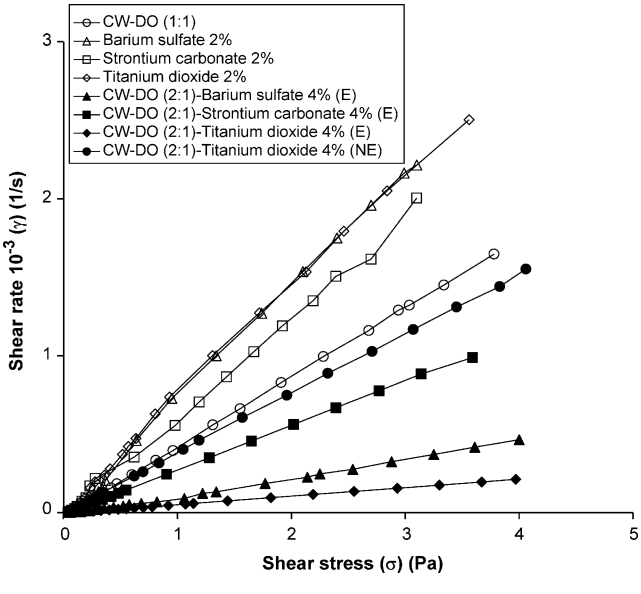

Fig. 1. Typical rheological behaviour of different formulations.

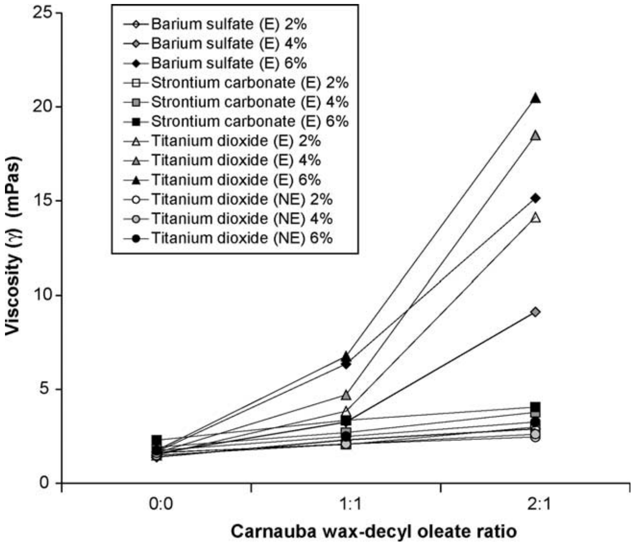

Fig. 2. Effect of the carnauba wax–decyl oleate ratio on the viscosity of the formulations.

4.2.4. Sun protection factor

The results of the in vitro sun protection factor (SPF) are depicted in Fig. 3. The tested pigments showed very low values after being dispersed alone in the formulations. To establish a comparison, the in vitro SPF of pigment free formulations having carnauba wax–decyl oleate at two different ratios, 1:1 and 2:1, were measured, and they presented SPFs between 2.2 and 4.5, respectively (data not shown in Fig. 1). Such values were even higher than those obtained by any other of the lipid free dispersions. The explanation could be found in the wax composition, which includes many potential UV absorbers, e.g. alkyl wax acid esters [23]. Nevertheless, the most interesting phenomenon can be appreciated when carnauba wax–decyl oleate nanoparticles were utilized for the encapsulation of pigments. An increase in SPF at different levels in the different formulations was identified. The formulations containing encapsulated barium sulfate and strontium carbonate at different concentrations, presented values no higher than eight. However, using titanium dioxide, elevated SPF values of about 50 were measured, particularly with the highest concentration of pigment. In the same figure, it is also noticed that the incorporation of titanium dioxide differed with the process.

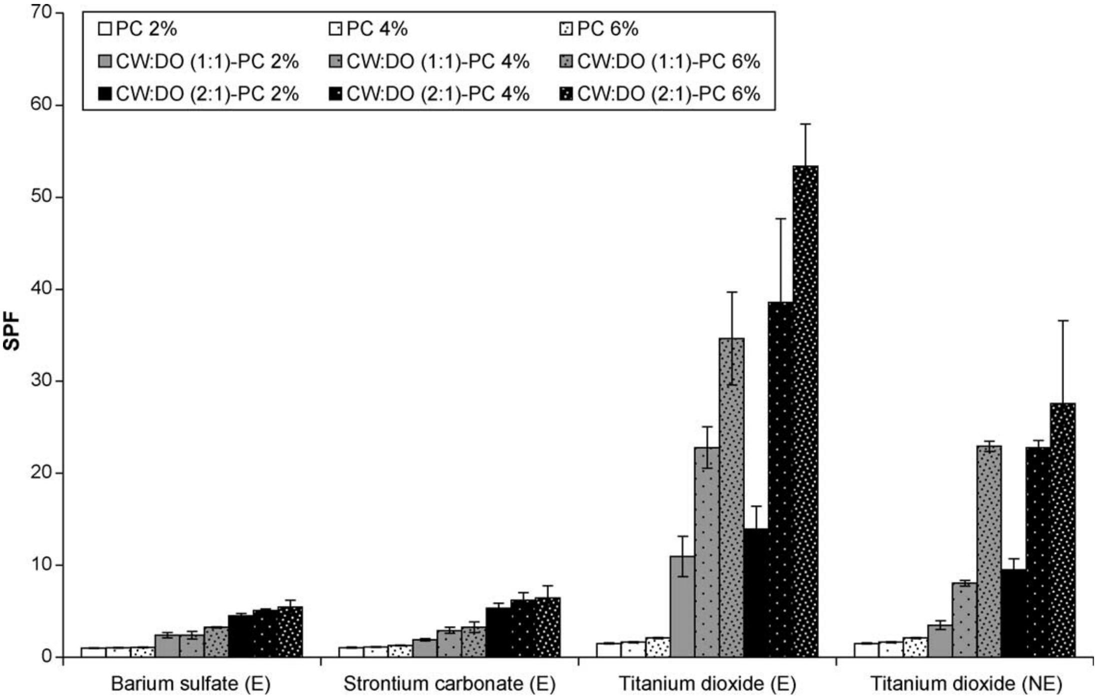

Fig. 3. Effect of pigment concentration, carnauba wax–decyl oleate ratio and manufacturing process on the sun protection factor (SPF). Key: CW, carnauba wax; DO, decyl oleate and PC, pigment concentration.

Just physical dispersion of the pigments in the presence of lipid matrices yielded lower SPFs than those of the simultaneous incorporation within them. In virtue of this, it could be concluded that the process of incorporation of titanium dioxide into the formulations established a difference in the performance of the SPF. The increases observed in the SPF might be explained by the applied lipid layers covering fully or partially the surface of pigments. Those modified pigments were responsible for the enhancement of phenomena such as UV-scattering, reflection and absorption closely related to the SPF at different grades. In other words, the obtained SPFs were probably justified by the achievement of larger particle sizes in the nanometric scale enabling to reach upper wavelengths in the UV-spectrum, and by the presence of more UV-absorbing substances attributed to the augmentation of wax loads. It must be also considered that lipid matrices contributed to obtain a better SPF, since they provided a fixation medium for the pigments when the nanosupensions were spread over the Transpore® tapes [24]. The viscosity values might confirm this observation since increased SPF values always coincided with higher viscosities (Figs. 1 and 2).

4.2.5. TEM characterization

The morphological characterization confirmed the information concerning to the mean particle size, as shown by the bars displayed on the figures (Figs. 4–7d). Typical carnauba wax–decyl oleate (1:1) nanoparticles can be visualized in Fig. 4. The surface of those particles seems to be integrated by many platelets, possibly formed after the accumulation of wax molecules during re-crystallization. In order to appreciate the changes experienced by the pigment crystal, photomicrographs of freely dispersed pigments were taken. Fig. 5a shows spherical crystals of a 2% barium sulfate dispersion in aqueous phase. The same figure shows some of the crystals presenting particle sizes close to those of their primary particles (PPS = 30 nm). On the right side (Fig. 5b), the same particles after the encapsulation are observed. It can be distinguished, that the flat rough surfaces originally

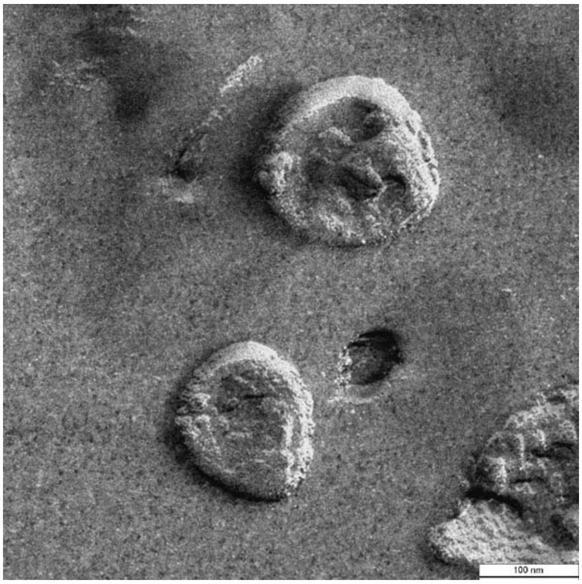

Fig. 4. TEM of a freeze fractured preparation of pigment free nanoparticles from formulation containing carnauba wax and decyl oleate in a ratio 1:1.

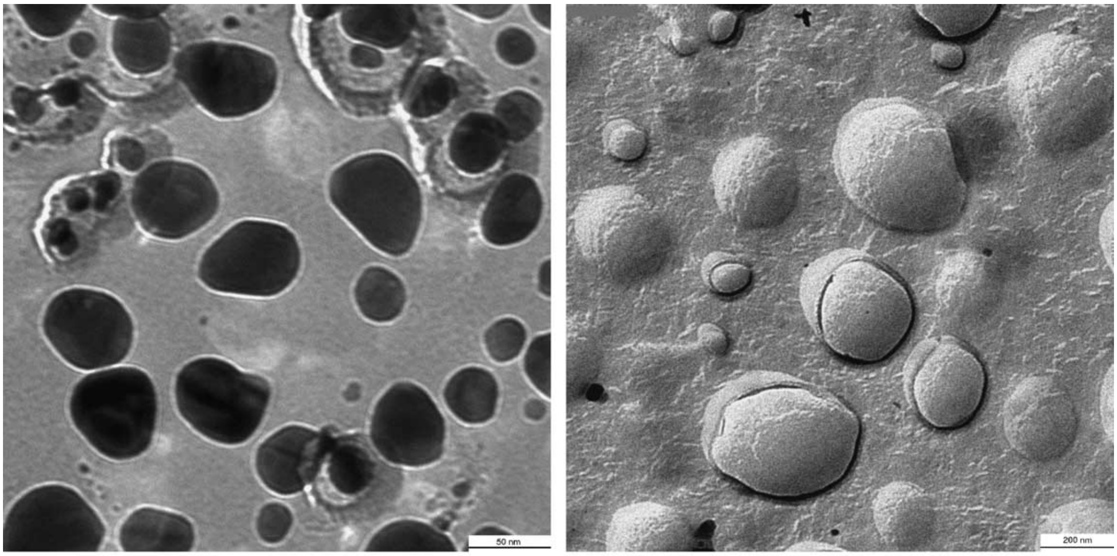

(a) (b)

Fig. 5. (a) TEM of a freeze fractured preparation of 2% (w/w) barium sulfate crystals freely dispersed in an aqueous phase. (b) TEM of a freeze fractured preparation of 2% (w/w) barium sulfate crystals encapsulated in a lipid matrix made up of carnauba wax–decyl oleate (1:1).

depicted in Fig. 4, were not longer found. This could be attributed to the location of crystals in the inner structure of the wax–oil matrices. For strontium carbonate, large agglomerates of about 1 μm consisting of many smaller spherical particles were identified in the aqueous dispersion as exemplified in Fig. 6a. However, after processing, deagglomeration seemed to occur and crystals were apparently covered by the lipids (Fig. 6b). Such phenomenon was reflected by a decrease not only in the mean particle sizes, but also in the polydispersity indices as seen in Table 1. For titanium dioxide, instead of a deagglomeration after pigment dispersion within lipids, a particle association could be described and large clumps of crystals were found in the matrix. However, conversely to what observed in the case of barium and strontium compounds, these crystals were not fully covered by the lipids, probably due to the irregular morphology of the agglomerates. The original needle crystals of titanium dioxide depicted in Fig. 7a could be still recognized on the matrices (Fig. 7b and c). Finally, as expected for a NE process, particle overlapping between titanium dioxide clumps and lipid particles could be easily observed (Fig. 7d).

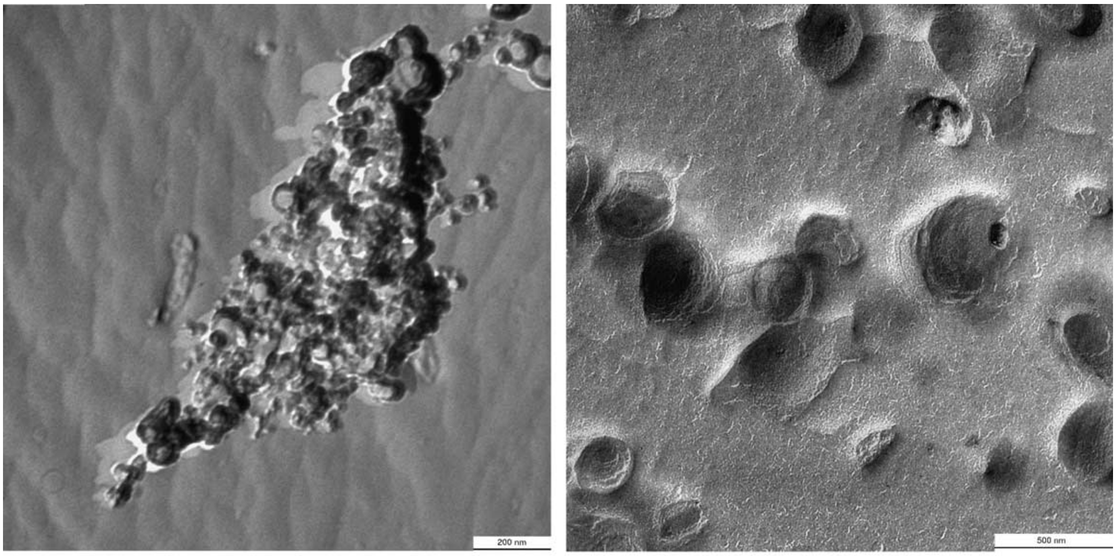

(a) (b)

Fig. 6. (a) TEM of a freeze fractured preparation of 2% (w/w) strontium carbonate agglomerates dispersed in an aqueous phase. (b) TEM of a freeze fractured preparation of 2% (w/w) strontium carbonate crystals encapsulated in a lipid matrix made up of carnauba wax–decyl oleate (2:1).

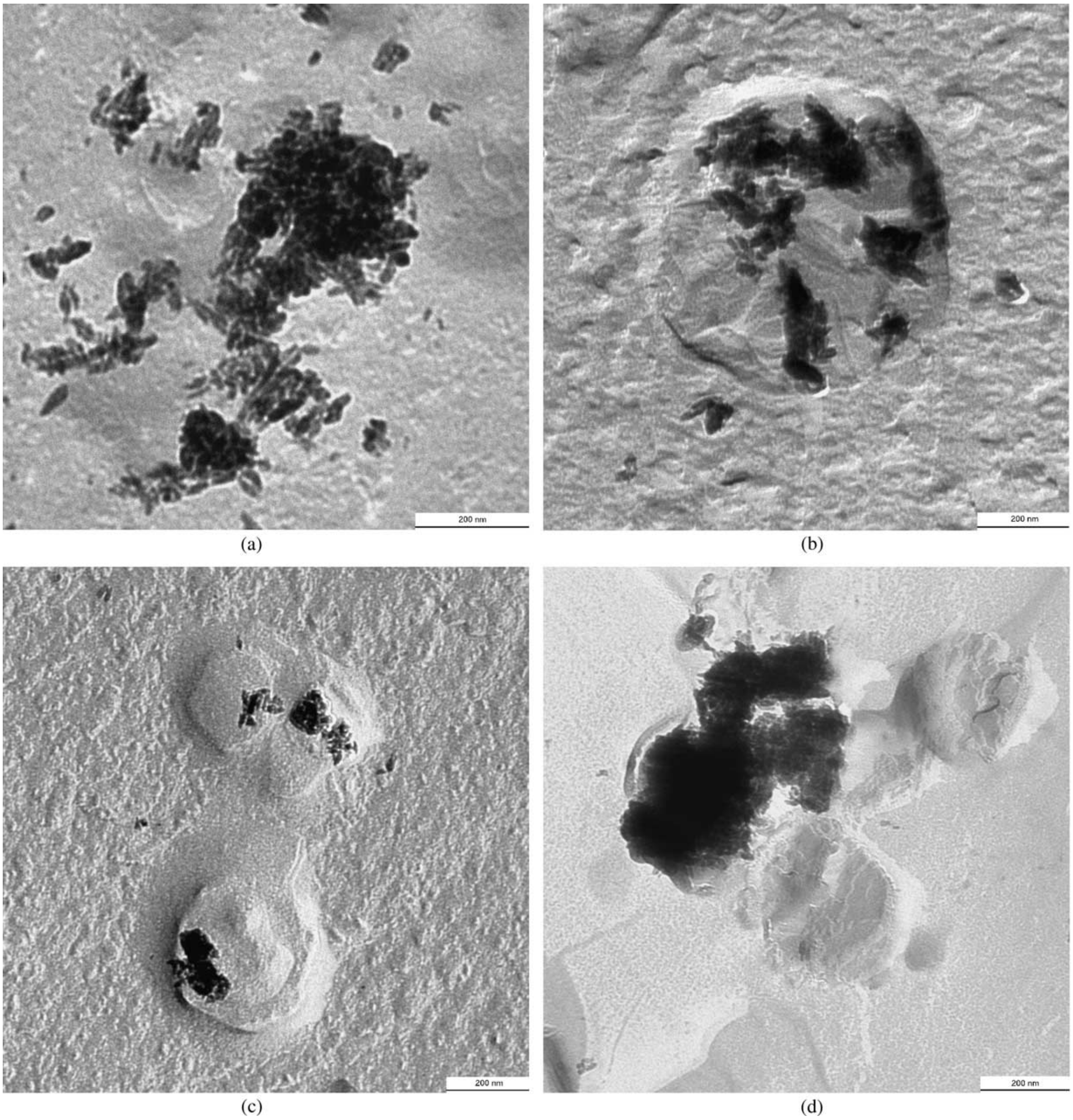

Fig. 7. (a) TEM of a freeze fractured preparation of 4% (w/w) titanium dioxide agglomerates dispersed in an aqueous phase. (b) TEM of a freeze fractured preparation of a nanoparticle containing 2% (w/w) titanium dioxide crystals encapsulated in a lipid matrix made up of carnauba wax–decyl oleate (1:1). (c) TEM of a freeze fractured preparation of carnauba wax–decyl oleate (1:1) nanoparticles containing 4% (w/w) titanium dioxide crystals apparently attached at the surface. (d) TEM of a freeze fractured preparation of nanoparticles on which, the titanium dioxide crystals 6% (w/w) were added after the cooling down of the lipid nanoparticle. The ratio carnauba wax to decyl oleate was 2:1.

4.2.6. Evaluation of nanosuspensions considering results from different characterization methods

The applied lipid matrices, showed to be compatible with the inorganic sunscreens since the incorporation of the latter into lipids presented no modification neither in the X-ray diffraction patterns of the carnauba wax–decyl oleate mixture nor in its thermal behavior. Furthermore, it was proven that in the nanosupensions, the obtained matrices used as adjuvants in the dispersion media contributed to the stabilization of the inorganic crystals in the aqueous suspensions. The purposed nanoparticles allowed to obtain, at a different extent depending on the nature of the applied inorganic sunscreens, increased SPFs. The SPFs of the formulations based on inorganic sunscreens showing UV absorption were particularly favored by the encapsulation within lipid matrices. This could be partially attributed to an increase in viscosity providing the pigments with a better fixation on the plates during the SPF measurements. Another phenomenon augmenting the SPF was an increase in particle size reinforcing the UV-blocking properties of the encapsulated substances. This could be supposed, since larger particle sizes always coincided with higher SPFs particularly when UV-absorbing inorganic sunscreens were used. Hence the better fixation of the crystals on the plates and the larger particle sizes obtained were factors contributing to a simultaneous enhancement of the scattering, reflection and absorption properties of titanium dioxide and carnauba wax when both substances were exposed together to the UV radiation. Conversely, those formulations consisting of compounds attenuating UV radiation mainly by scattering and reflection were signaled to be less effective, since they showed only small increases in their SPFs explained only by the use of higher carnauba wax loads.

5. Conclusion

The use of nanoparticles consisting of matrices based on a mixture between a solid lipid, carnauba wax, and a liquid lipid, decyl oleate, as carriers for inorganic nanocrystals seems to be a promising technology for future sunscreen formulations. The encapsulation of the tested inorganic compounds enhanced the intrinsic SPF of those substances. Titanium dioxide was particularly favored by this process in virtue of its UV-absorption capacity. The used mixed lipid matrices positively affected the viscosity of the systems giving the formulations a better fixation after being applied on plates for the SPF measurement. According to the *z*-potential values, the stability of the formulation was favored in all the cases by the use of wax–oil matrices. The efficiency of the encapsulation rate has to be evaluated in an upcoming study.

Acknowledgements

Deutscher Akademischer Austauschdienst (DAAD) is thanked for the fellowship to R. Villalobos. Mr Dipl. Ing. Ebenau from the Department of Process and Systems Engineering of the University of Magdeburg is thanked for his assistance during the zeta potential measurements. The companies, Solvay GmbH, Kemira OY and Brenntag GmbH, are thanked for the kind donation of substances.

References

[1] R. Bissonnette, Update on sunscreens, Skin Ther. Lett. 2 (5) (1997) 2–5.

[2] R.M. Sayre, N. Kollias, R. Roberts, A. Baqer, Physical sunscreens, J. Soc. Cosmet. Chem. 41 (March–April) (1990) 103–109.

[3] Barium Strontium SBU. Solvay-Chemicals Bull, 2003.

[4] G.S. Hahn, Strontium is a potent and selective inhibitor of sensory irritation, Dermatol. Surg. 25 (9) (1999) 689–693.

[5] H. Zhai, W. Hannon, G.S. Hahn, A. Pelossi, R. Harper, H. Maibach, Strontium nitrate supresses chemically-induced sensory irritation in humans, Contact Dermat. 42 (2) (2000) 98–100.

[6] N. Kollias, A. Baqer, K. Razi Naqvi, Fiber optic spectrophotometer for noninvasive transmission and diffuse reflection studies, Spectrosc. Lett. 19 (1986) 149–150.

[7] G.H. Dahms, Formulating with a physical sun block, in: R. Schüller, P. Romanowski (Eds.), Beginning Cosmetic Chemistry, Allured Publishing Corp., Carol Stream, IL, 1998, pp. 159–169.

[8] D. Fairhurst, M.A. Mitchnick, Particulate sun blocks, in: N.J. Lowe, N.A. Shaath, M.A. Pathak (Eds.), General Principles in Sunscreens: Development, Evaluation and Regulatory Aspects, Marcel Dekker, New York, NY, 1997, pp. 313–352.

[9] D. Fairhurst, Surface coating and the optimization of microfine oxides in sunscreens formulations, in: R. Schüller, P. Romanowski (Eds.), Beginning Cosmetic Chemistry, Allured Publishing Corp., Carol Stream, IL, 1998, pp. 147–158.

[10] UV-Titan M160. Product Data Sheet. Kemira Pigments. 10/2000.

[11] A. Ramdoska, R.H. Müller, The Chemical Stability of the Lipid Matrices of Solid Lipid Nanoparticles (SLN), Proceedings of Fourth World Meeting ADRITELF/APGI/APV, Florence, 8/11, April, 2002, pp. 683–684.

[12] K. Westesen, H. Bunjes, M.H.J. Koch, Physicochemical characterization of liquid nanoparticles and evaluation of their loading capacity and sustained realease potential, J. Control. Release 48 (1997) 223–226.

[13] R.H. Müller, M. Radtke, S.A. Wissing, Solid lipid nanoparticles (SLN) and nanostructured lipid carriers (NLC) in cosmetic and dermatological preparations, Adv. Drug Deliv. Rev. 54 (Suppl. 1) (2002) 131–155.

[14] V. Jenning, A.F. Thünemann, S.H. Gohla, Characterisation of a novel solid liquid nanoparticle carrier system based on binary mixtures of liquid and solid lipids, Int. J. Pharm. 199 (2000) 167–177.

[15] R.A. Bodmeier, Waxes, in: Encyclopedia Phamaceutical Technology, Marcel Dekker, New York, NY, 2002, pp. 2988–2999.

[16] Cetiol® V. Product Description. Cognis Care Chemicals Bull, 2002.

[17] R.H. Müller, B.H.L. Böhm, Dispersion techniques for laboratory and industrial scale processing, Wissenschaftliche Verlagsgesellschaft mbH Stuttgart (2001) 77–87.

[18] N. Kollias, The absorption properties of physical sunscreens, Arch. Dermatol. 135 (2) (1999) 209–210.

[19] R.H. Müller, R. Schumann, Teilchengrössenmessung in der Laborpraxis, Wissenschaftliche Verlagsgesellschaft mbH Stuttgart (1996) 25–45.

[20] T.M. Riddick, Zeta-Meter Manual, Zeta-Meter, Inc., New York, NY, 1968.

[21] H.D. Tcheusschner, Grundlegende rheologische Eigenschaften, in: D. Weipert, H.D. Tscheuschner, E. Windhab (Eds.), Rheologie der Lebensmittel, Behr's Verlag GmbH, 1993, pp. 51–100.

[22] R.H. Müller, Zetapotential und Partikelladung in der Laborpraxis, Wissenschaftliche Verlagsgesselschaft mbH Stuttgart 1996; 45–52.

[23] I. Basson, E.C. Reynhardt, An investigation of the structures and molecular dynamics of natural waxes: II. Carnauba wax, J. Phys. D: Appl. Phys. 21 (1988) 1429–1433.

[24] M.W. Anderson, J.P. Hewitt, S.R. Spruce, Broad-spectrum physical sunscreens: titanium dioxide and zinc dioxide, in: N.J. Lowe, N.A. Shaath, M.A. Pathak (Eds.), General Principles in Sunscreens: Development, Evaluation and Regulatory Aspects, Marcel Dekker, New York, NY, 1997, pp. 353–398.